Increased upconversion quantum yield in photonic structures due to local field enhancement and modification of the local density of states – a simulation-based analysis

Barbara Herter,[1,*] Sebastian Wolf,[1] Stefan Fischer,[1] Johannes Gutmann,[1] Benedikt Bläsi,[1] and Jan Christoph Goldschmidt[1,2]

[1]*Fraunhofer Institute for Solar Energy Systems, Heidenhofstr. 2, 79110 Freiburg, Germany*
[2]*Department of Physics, Imperial College, London SW7 2AZ, United Kingdom*
**barbara.herter@ise.fraunhofer.de*

Abstract: In upconversion processes, two or more low-energy photons are converted into one higher-energy photon. Besides other applications, upconversion has the potential to decrease sub-band-gap losses in silicon solar cells. Unfortunately, upconverting materials known today show quantum yields, which are too low for this application. In order to improve the upconversion quantum yield, two parameters can be tuned using photonic structures: first, the irradiance can be increased within the structure. This is beneficial, as upconversion is a non-linear process. Second, the rates of the radiative transitions between ionic states within the upconverter material can be altered due to a varied local density of photonic states. In this paper, we present a theoretical model of the impact of a photonic structure on upconversion and test this model in a simulation based analysis of the upconverter material β-$NaYF_4$:20% Er^{3+} within a dielectric waveguide structure. The simulation combines a finite-difference time-domain simulation model that describes the variations of the irradiance and the change of the local density of photonic states within a photonic structure, with a rate equation model of the upconversion processes. We find that averaged over the investigated structure the upconversion luminescence is increased by a factor of 3.3, and the upconversion quantum yield can be improved in average by a factor of 1.8 compared to the case without the structure for an initial irradiance of 200 Wm^{-2}.

OCIS codes: (190.7220) Upconversion; (350.4238) Nanophotonics and photonic crystals; (350.2770) Gratings; (130.5296) Photonic crystal waveguides.

References and links

1. F. Wang and X. Liu, "Recent advances in the chemistry of lanthanide-doped upconversion nanocrystals," Chem. Soc. Rev. **38**, 976–989 (2009).
2. M. Wang, C.-C. Mi, J.-L. Liu, X.-L. Wu, Y.-X. Zhang, W. Hou, F. Li, and S.-K. Xu, "One-step synthesis and characterization of water-soluble $NaYF_4$:Yb,Er/polymer nanoparticles with efficient up-conversion fluorescence," J. Alloys Compd. **485**, L24–7 (2009).

#192534 - $15.00 USD Received 18 Jun 2013; revised 21 Jul 2013; accepted 21 Jul 2013; published 28 Aug 2013

3. H. S. Qian, H. C. Guo, P. C.-L. Ho, R. Mahendran, and Y. Zhang, "Mesoporous-silica-coated up-conversion fluorescent nanoparticles for photodynamic therapy," Small **5**, 2285–2290 (2009).
4. D. K. Chatterjee, A. J. Rufaihah, and Y. Zhang, "Upconversion fluorescence imaging of cells and small animals using lanthanide doped nanocrystals," Biomaterials **29**, 937 – 943 (2008).
5. B. Richards, "Enhancing the performance of silicon solar cells via the application of passive luminescence conversion layers," Sol. Energy Mater. Sol. Cells **90**, 2329 – 2337 (2006).
6. F. Auzel, "Upconversion and anti-stokes processes with f and d ions in solids," Chem. Rev. **104**, 139–174 (2004).
7. S. Fischer, J. C. Goldschmidt, P. Löper, G. H. Bauer, R. Brüggemann, K. Krämer, D. Biner, M. Hermle, and S. W. Glunz, "Enhancement of silicon solar cell efficiency by upconversion: Optical and electrical characterization," J. Appl. Phys. **108**, 044912 (2010).
8. B. Richards and A. Shalav, "Enhancing the near-infrared spectral response of silicon optoelectronic devices via up-conversion," IEEE Trans. Electron Devices **54**, 2679 –2684 (2007).
9. J. Goldschmidt, S. Fischer, P. Löper, K. Krämer, D. Biner, M. Hermle, and S. Glunz, "Experimental analysis of upconversion with both coherent monochromatic irradiation and broad spectrum illumination," Sol. Energy Mater. Sol. Cells **95**, 1960 – 1963 (2011).
10. M. Pollnau, D. R. Gamelin, S. R. Lüthi, H. U. Güdel, and M. P. Hehlen, "Power dependence of upconversion luminescence in lanthanide and transition-metal-ion systems," Phys. Rev. B **61**, 3337–3346 (2000).
11. F. Hallermann, C. Rockstuhl, S. Fahr, G. Seifert, S. Wackerow, H. Graener, G. v. Plessen, and F. Lederer, "On the use of localized plasmon polaritons in solar cells," Phys. Status Solidi A **205**, 2844–2861 (2008).
12. F. Hallermann, J. C. Goldschmidt, S. Fischer, P. Löper, and G. von Plessen, "Calculation of up-conversion photoluminescence in Er^{3+} ions near noble-metal nanoparticles," in "Proc. SPIE Vol. 7725, 77250Y," (2010), Photonics for Solar Energy Systems III.
13. S. Fischer, F. Hallermann, T. Eichelkraut, G. von Plessen, K. W. Krämer, D. Biner, H. Steinkemper, M. Hermle, and J. C. Goldschmidt, "Plasmon enhanced upconversion luminescence near gold nanoparticles - simulation and analysis of the interactions," Opt. Express **20**, 271–82 (2012).
14. S. Fischer, F. Hallermann, T. Eichelkraut, G. von Plessen, K. W. Krämer, D. Biner, H. Steinkemper, M. Hermle, and J. C. Goldschmidt, "Plasmon enhanced upconversion luminescence near gold nanoparticles; simulation and analysis of the interactions: Errata," Opt. Express **21**, 10606–10606 (2013).
15. H. Mertens and A. Polman, "Plasmon-enhanced erbium luminescence," Appl. Phys. Lett. **89**, 211107 (2006).
16. S. Schietinger, T. Aichele, H.-Q. Wang, T. Nann, and O. Benson, "Plasmon-enhanced upconversion in single $NaYF_4$:Yb^{3+}/Er^{3+} codoped nanocrystals," Nano Lett. **10**, 134–138 (2010). PMID: 20020691.
17. E. Dulkeith, A. C. Morteani, T. Niedereichholz, T. A. Klar, J. Feldmann, S. A. Levi, F. C. J. M. van Veggel, D. N. Reinhoudt, M. Möller, and D. I. Gittins, "Fluorescence quenching of dye molecules near gold nanoparticles: Radiative and nonradiative effects," Phys. Rev. Lett. **89**, 203002 (2002).
18. J. C. Goldschmidt, S. Fischer, H. Steinkemper, B. Herter, T. Rist, S. Wolf, B. Blasi, F. Hallermann, G. von Plessen, K. W. Kramer, D. Biner, and M. Hermle, "Increasing upconversion by metal and dielectric nanostructures," in "Proceedings of SPIE," , vol. 8256, A. Freundlich and J.-F. F. Guillemoles, eds. (SPIE, 2012), vol. 8256, pp. 825602–1–9.
19. S. Wolf, B. Herter, S. Fischer, O. Höhn, R. Martn-Rodrguez, U. Aeberhard, and J. Goldschmidt*, "Exploiting photonic structures to improve the efficiency of upconversion by field enhancement and a modification of the local density of photonic states," in "Proceedings of the 27th European Photovoltaic Solar Energy Conference and Exhibition," (Frankfurt, 2012).
20. S. John and T. Quang, "Spontaneous emission near the edge of a photonic band gap," Phys. Rev. A **50**, 1764–1769 (1994).
21. W. L. Vos, A. F. Koenderink, and I. S. Nikolaev, "Orientation-dependent spontaneous emission rates of a two-level quantum emitter in any nanophotonic environment," Phys. Rev. A **80**, 053802 (2009).
22. E. Yablonovitch, "Inhibited spontaneous emission in solid-state physics and electronics," Phys. Rev. Lett. **58**, 2059–2062 (1987).
23. S. G. Romanov, A. V. Fokin, and R. M. D. L. Rue, "Eu^{3+} emission in an anisotropic photonic band gap environment," Appl. Phys. Lett. **76**, 1656–1658 (2000).
24. C. A. Foell, E. Schelew, H. Qiao, K. A. Abel, S. Hughes, F. C. J. M. van Veggel, and J. F. Young, "Saturation behaviour of colloidal PbSe quantum dot exciton emission coupled into silicon photonic circuits," Opt. Express **20**, 10453–10469 (2012).
25. D. Englund, D. Fattal, E. Waks, G. Solomon, B. Zhang, T. Nakaoka, Y. Arakawa, Y. Yamamoto, and J. Vučković, "Controlling the spontaneous emission rate of single quantum dots in a two-dimensional photonic crystal," Phys. Rev. Lett. **95**, 013904 (2005).
26. F. Zhang, Y. Deng, Y. Shi, R. Zhang, and D. Zhao, "Photoluminescence modification in upconversion rare-earth fluoride nanocrystal array constructed photonic crystals," J. Mater. Chem. **20**, 3895–3900 (2010).
27. Z. Yang, K. Zhu, Z. Song, D. Zhou, Z. Yin, and J. Qiu, "Effect of photonic bandgap on upconversion emission in $YbPO_4$:Er inverse opal photonic crystals," Appl. Opt. **50**, 287–290 (2011).
28. M. J. A. de Dood, A. Polman, and J. G. Fleming, "Modified spontaneous emission from erbium-doped photonic layer-by-layer crystals," Phys. Rev. B **67**, 115106 (2003).

#192534 - $15.00 USD Received 18 Jun 2013; revised 21 Jul 2013; accepted 21 Jul 2013; published 28 Aug 2013

29. H. A. Lopez and P. M. Fauchet, "Erbium emission from porous silicon one-dimensional photonic band gap structures," Appl. Phys. Lett. **77**, 3704 –3706 (2000).
30. C. M. Johnson, P. J. Reece, and G. J. Conibeer, "Slow-light-enhanced upconversion for photovoltaic applications in one-dimensional photonic crystals," Opt. Lett. **36**, 3990–3992 (2011).
31. C. Johnson, P. Reece, and G. Conibeer, "Theoretical and experimental evaluation of silicon photonic structures for enhanced erbium up-conversion luminescence," Sol. Energy Mater. Sol. Cells **112**, 168 – 181 (2013).
32. M. Liscidini and L. C. Andreani, "Highly efficient second-harmonic generation in doubly resonant planar microcavities," Appl. Phys. Lett. **85**, 1883–1885 (2004).
33. A. Rodriguez, M. Soljacic, J. D. Joannopoulos, and S. G. Johnson, "$\chi(2)$ and $\chi(3)$ harmonic generation at a critical power in inhomogeneous doublyresonant cavities," Opt. Express **15**, 7303–7318 (2007).
34. A. Hayat and M. Orenstein, "Photon conversion processes in dispersive microcavities: Quantum-field model," Phys. Rev. A **77**, 013830 (2008).
35. K. Rivoire, Z. Lin, F. Hatami, W. T. Masselink, and J. Vučković, "Second harmonic generation in gallium phosphide photonic crystal nanocavities with ultralow continuous wave pump power," Opt. Express **17**, 22609–22615 (2009).
36. K. Rivoire, S. Buckley, and J. Vučković, "Multiply resonant photonic crystal nanocavities for nonlinear frequency conversion," Opt. Express **19**, 22198–22207 (2011).
37. N. Liu, W. Qin, G. Qin, T. Jiang, and D. Zhao, "Highly plasmon-enhanced upconversion emissions from Au@β - $NaYF_4$:Yb,Tm hybrid nanostructures," Chem. Commun. **47**, 7671–7673 (2011).
38. H. P. Paudel, L. Zhong, K. Bayat, M. F. Baroughi, S. Smith, C. Lin, C. Jiang, M. T. Berry, and P. S. May, "Enhancement of near-infrared-to-visible upconversion luminescence using engineered plasmonic gold surfaces," J. Phys. Chem. C **115**, 19028–19036 (2011).
39. A. F. Oskooi, D. Roundy, M. Ibanescu, P. Bermel, J. Joannopoulos, and S. G. Johnson, "Meep: A flexible free-software package for electromagnetic simulations by the FDTD method," Comput. Phys. Commun. **181**, 687 – 702 (2010).
40. S. S. Wang and R. Magnusson, "Multilayer waveguide-grating filters," Appl. Opt. **34**, 2414–2420 (1995).
41. J. Nishii, K. Kintaka, and T. Nakazawa, "High-efficiency transmission gratings buried in a fused-sio2 glass plate," Appl. Opt. **43**, 1327–1330 (2004).
42. K. W. Krämer, D. Biner, G. Frei, H. U. Güdel, M. P. Hehlen, and S. R. Lüthi, "Hexagonal sodium yttrium fluoride based green and blue emitting upconversion phosphors," Chem. Mater. **16**, 1244–1251 (2004).
43. R. E. Thoma, H. Insley, and G. M. Hebert, "The sodium fluoride-lanthanide trifluoride systems," Inorg. Chem. **5**, 1222–9 (1966).
44. E. Snoeks, G. N. van den Hoven, A. Polman, B. Hendriksen, M. B. J. Diemeer, and F. Priolo, "Cooperative upconversion in erbium-implanted soda-lime silicate glass optical waveguides," J. Opt. Soc. Am. B **12**, 1468–1474 (1995).
45. M. Fox, *Quantum Optics* (Oxford University, 2006).
46. P. Bermel, A. Rodriguez, J. D. Joannopoulos, and M. Soljacic, "Tailoring optical nonlinearities via the Purcell effect," Phys. Rev. Lett. **99**, 053601 (2007).
47. C. Hermann and O. Hess, "Modified spontaneous-emission rate in an inverted-opal structure with complete photonic bandgap," J. Opt. Soc. Am. B **19**, 3013–3018 (2002).
48. J.-K. Hwang, H.-Y. Ryu, and Y.-H. Lee, "Spontaneous emission rate of an electric dipole in a general microcavity," Phys. Rev. B **60**, 4688–4695 (1999).
49. J. C. Goldschmidt, *Novel solar cell concepts* (Verlag Dr. Hut, München, 2010).
50. S. Fischer, H. Steinkemper, P. Löper, M. Hermle, and J. C. Goldschmidt, "Modeling upconversion of erbium doped microcrystals based on experimentally determined Einstein coefficients," J. Appl. Phys. **111**, 013109 (2012).
51. M. J. A. de Dood, J. Knoester, A. Tip, and A. Polman, "Förster transfer and the local optical density of states in erbium-doped silica," Phys. Rev. B **71**, 115102 (2005).
52. C. Blum, N. Zijlstra, A. Lagendijk, M. Wubs, A. P. Mosk, V. Subramaniam, and W. L. Vos, "Nanophotonic control of the Förster resonance energy transfer efficiency," Phys. Rev. Lett. **109**, 203601 (2012).
53. P. Andrew and W. L. Barnes, "Förster energy transfer in an optical microcavity," Science **290**, 785–788 (2000).
54. J. C. Goldschmidt, P. Löper, S. Fischer, S. Janz, M. Peters, S. W. Glunz, G. Willeke, E. Lifshitz, K. Krämer, and D. Biner, "Advanced upconverter systems with spectral and geometric concentration for high upconversion efficiencies," in "Proceedings IUMRS International Conference on Electronic Materials," (2008), pp. 307–11.
55. C. Strümpel, M. McCann, C. del Canizo, I. Tobias, and P. Fath, "Erbium-doped up-converters of silicon solar cells: assessment of the potential," in "Proceedings of the 20th European Photovoltaic Solar Energy Conference," (2005), pp. 43–6.
56. K. Forberich, A. Gombert, S. Pereira, J. Crewett, U. Lemmer, M. Diem, and K. Busch, "Lasing mechanisms in organic photonic crystal lasers with two-dimensional distributed feedback," J. Appl. Phys. **100**, 023110 (2006).
57. S. Riechel, C. Kallinger, U. Lemmer, J. Feldmann, A. Gombert, V. Wittwer, and U. Scherf, "A nearly diffraction limited surface emitting conjugated polymer laser utilizing a two-dimensional photonic band structure," Appl. Phys. Lett. **77**, 2310–2312 (2000).

#192534 - $15.00 USD Received 18 Jun 2013; revised 21 Jul 2013; accepted 21 Jul 2013; published 28 Aug 2013

1. Introduction

Upconverter materials convert two or more low-energy photons into one higher-energy photon. Among other applications [1–4], upconversion could be used to increase the efficiency of solar cells. Here, two or more photons with energies below the band gap of the used semiconductor material are absorbed within the upconverter and one photon with an energy above the band gap is emitted. This photon can subsequently be utilized by the solar cell. For silicon solar cells, the transmission losses due to sub-band-gap photons correspond to 20% of the incident solar energy [5], which could be harvested using upconversion [6].

An effect of upconversion on the external quantum efficiency of a solar cell has already been demonstrated for the application of the upconverter material β-$NaYF_4$ doped with 20% erbium [7–9] attached to the rear of a bifacial silicon solar cell. The external quantum efficiency of the solar cell upconverter device was measured and a response was shown in the absorption range of the upconverter around 1520 nm. Unfortunately, the observed effect is relatively small, with a measured external quantum efficiency of 0.34% [7] or 3.4% [8] at different excitation levels. To make upconversion an approach useful for photovoltaics, upconversion quantum yields need to be increased. It has been shown that an increased irradiance increases the upconversion luminescence [10] due to the non-linearity of the process.

One possibility to increase the irradiance on the upconverter material is the exploitation of plasmonic effects in noble metal nanoparticles, which can cause a high local field enhancement [11–14] around the metallic particles. This enhancement has to be shown to be able to increase the erbium photoluminescence [15]. The effect on the upconversion luminescence has been shown by Schietinger et al., they measured an increased by a factor of 3.8 in the proximity of a single gold nanoparticle [16]. However, the coupling to the nanoparticle can lead to parasitic absorptions within the metal [17]. While there might still be unexplored complex plasmonic structures in which these parasitic absorptions are overcompensated by extremely high field enhancements, such parasitic absorption can in principle be avoided by using dielectric nanostructures [18, 19].

The conventional photoluminescence (emission wavelength longer than the absorption wavelength) in photonic structures has been thoroughly investigated [20–22]. Additionally, the photoluminescence of rare-earth ions and luminescent quantum dots incorporated in photonic crystal environments has already been investigated experimentally, for example in [23–29]. The erbium emission at a wavelength of 1.5 μm can be suppressed in a suitable photonic crystal environment [28] or enhanced and tuned in a one-dimensional photonic band gap environment [29]. There has also been experimental evidence that upconversion luminescence (emission wavelength shorter than the absorption wavelength) can be increased for erbium embedded in Bragg stacks produced from porous silicon layers [30, 31].

Considering upconversion processes, a lot of work has been done on second and third harmonic generation in a cavity structure which has been investigated theoretically [32–34] and experimentally [35, 36]. These processes require coherent, monochromatic light. Here, as we are interested in a solar cell application, we want to focus on upconversion in erbium, which relies on ground state absorption, excited state absorption and energy transfer upconversion. Thus, upconversion in this material is also possible under broad-band excitation.

Upconversion is more complex than the conventional photoluminescence as more than one photon is involved in the excitation. Therefore, upconversion is a non-linear process and the irradiance at the position of the upconverter is an important parameter, additional to factors such as the local density of photonic states at the transition frequencies and the transition probabilities between the ionic states of the upconverter material.

In this paper, we seek to provide a theoretical description of upconversion based on ground and excited state absorption and energy transfer upconversion in photonic structures and present

#192534 - $15.00 USD Received 18 Jun 2013; revised 21 Jul 2013; accepted 21 Jul 2013; published 28 Aug 2013

first results of our analysis using a combination of different simulation models. Our special interest will be on how the different effects can be utilized to increase upconversion quantum yields. In Section 2, we will introduce a theoretical description of the different effects and present simulation models for the determination of the irradiance enhancement, the change of the local density of photonic states affecting the emission processes and a rate equation model describing the upconverter material β-$NaYF_4$ doped with 20% Er^{3+}. In Section 3, we present the results obtained by applying these models to a grating-waveguide test structure. In Section 4, we will discuss our findings and eventually conclude the paper in Section 5.

2. Methods

2.1. Irradiance enhancement

As mentioned above, several different effects have to be considered when analyzing the effect of photonic structures on upconversion. The first one is the flux of incoming photons $\Phi_{in}(\vec{r},\omega_{in})$ at the position $\vec{r}$ of the upconverter with a frequency ω_{in} such that the photons can be absorbed by the upconverter. The stimulated processes of ground state absorption (GSA), excited state absorption (ESA), and stimulated emission (STE), scale with the incoming photon flux density [37, 38]. In the following, GSA, ESA and STE are matrices describing the probabilities of the respective transitions between electronic levels of an upconverting material. The matrices with the index '0' describe the undisturbed system whereas those with the index 'struct' describe the same processes in the presence of a photonic structure. This can be expressed as:

$$\begin{aligned} GSA_{\text{struct}}(\vec{r}) &= \gamma_{\text{E}}(\vec{r}) \times GSA_0 \\ ESA_{\text{struct}}(\vec{r}) &= \gamma_{\text{E}}(\vec{r}) \times ESA_0 \\ STE_{\text{struct}}(\vec{r}) &= \gamma_{\text{E}}(\vec{r}) \times STE_0, \end{aligned} \tag{1}$$

where $\gamma_E(\vec{r})$ is the factor by which the photon flux $\Phi(\vec{r})$ at the position $\vec{r}$ of the upconverter changes due to the photonic structure:

$$\gamma_{\text{E}}(\vec{r}) = \frac{\Phi_{\text{in,struct}}(\vec{r},\omega_{\text{in}})}{\Phi_{\text{in,0}}(\vec{r},\omega_{\text{in}})}. \tag{2}$$

The indices 'struct' and '0' again indicate the case with and without the photonic structure, respectively.

2.2. Simulation of the irradiance enhancement

The enhancement of the irradiance γ_{E} is determined using Meep, a freely available software package for finite-difference time-domain (FDTD)-simulations [39]. In this paper, we present results obtained for a grating-waveguide structure as sketched in Fig. 1. Similar structures have been investigated for example in [40, 41].

They have the advantage, that considerable irradiance enhancement factors can be reached within and that they offer a great flexibility for optimization, thus we used it as a test structure for our methodology.

The presented structure was illuminated by an infinitely extended line source. The source emits at a wavelength of 1523 nm. The illumination with TE- and TM-polarized waves was simulated simultaneously. The source was placed at a distance of ten times the emission wavelength from the structure, such that the emission from the line source is not affected by the presence of the structure. This setting corresponds to the case of planar waves illuminating the structure. For our model system, we assumed the use of β-$NaYF_4$ doped with 20% Er^{3+} as upconverter material. This material shows very efficient upconversion of photons from the near

#192534 - $15.00 USD Received 18 Jun 2013; revised 21 Jul 2013; accepted 21 Jul 2013; published 28 Aug 2013

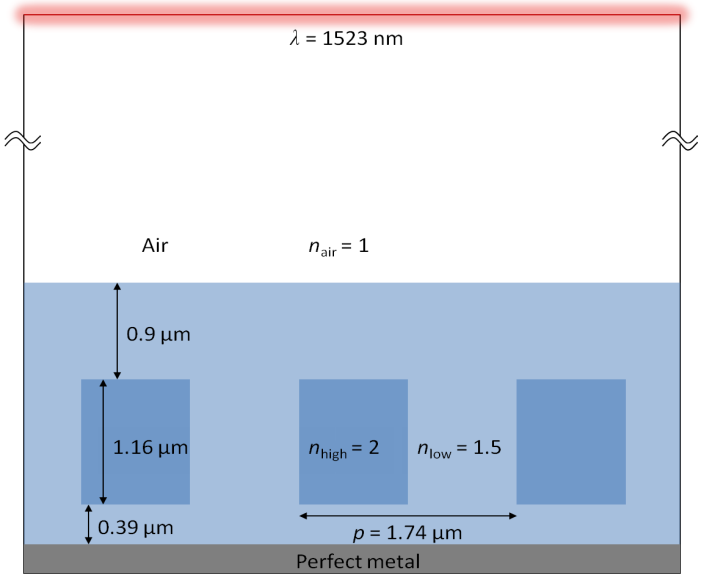

Fig. 1. Simulated grating-waveguide structure with an optimized period of 1.74 μm, a grating height of 1.16 μm, a layer below the grating with a height of 0.39 μm and a top layer thickness of 0.9 μm. The refractive indices n_{high} and n_{low} used for the simulation are 2 and 1.5, respectively. The infinitely extended line source is sketched by the red, glowing region above the structure.

infrared to energies above the band gap of silicon [42]. Efficient upconversion is observed for an excitation wavelength of 1523 nm. Therefore, this wavelength was chosen for the emission of the source. The refractive index of Er^{3+}-doped β-$NaYF_4$ has been reported to be $n = 1.48$ [43] and $n = 1.52$ [8]. In our grating waveguide test structure, a matching refractive index n_{low} of 1.5 was assumed for the simulation. For the higher refractive index region a refractive index $n_{\text{high}} = 2$ was chosen, a value that could be achieved with TiO_2, or a-SiC, for example. In this case, the upconverter is placed only in the low-index part of the structure. On the other hand, one can also imagine implanting erbium ions into the whole structure. This has been shown to be possible in principle by Snoeks et al. and Mertens et al. [15,44] although in these works, the erbium luminescence is investigated and upconversion was considered a loss-mechanism. As this ion-implantation presents the possibility to dope the whole structure with erbium, we will analyze the different effects for the high-index region of the grating, as well.

At this point it has to be noted that for the FDTD simulations we do not consider any absorption inside the waveguide structure, which corresponds to a low doping of the structure with upconverter material and ideal material properties for the whole structure. The simulations were carried out in a two-dimensional setup. In x-direction, periodic boundaries were implemented, corresponding to a structure that extends infinitely into this direction. Above the structure and the source, infinitely extended space is assumed. This is simulated using an absorbing perfectly matched layer (PML).

For a specific wavelength, the photon flux is proportional to the time-averaged irradiance I. This irradiance is more easily accessible from the simulation data and can be extracted from the simulation after a steady state is reached.

The irradiance at the position $\vec{r}$ is determined according to:

#192534 - $15.00 USD Received 18 Jun 2013; revised 21 Jul 2013; accepted 21 Jul 2013; published 28 Aug 2013

$$I(\vec{r}) = n \times E(\vec{r})^2, \tag{3}$$

with E being the electric field component. The altered irradiance $I_{\text{struct}}(\vec{r})$ within the structure is compared to the irradiance I_0 obtained for the same line source placed in a homogeneous medium with the refractive index of the upconverter ($n_0 = 1.5$). Meep, the FDTD-implementation used here, supports the calculation of complex fields [39]. The complex field vector is proportional to the time-average of the field amplitude, so the complex field vector is analyzed to determine the change in the time-averaged irradiance. The fields are recorded once the steady-state field distribution is reached after the plane wave illumination has been switched on. This steady-state situation is reached after the wave has propagated twice through the structure and another 100 periods of the incident light have passed.

The local enhancement factor $\gamma_{\text{E}}(\vec{r})$ is obtained by relating the two simulation results of the structure and the homogeneous reference to each other:

$$\gamma_E(\vec{r}) = \frac{n_{\text{struct}}(\vec{r})}{n_0} \times \frac{I_{\text{struct}}(\vec{r})}{I_0(\vec{r})} = \frac{n_{\text{struct}}(\vec{r})}{n_0} \times \left(\frac{E_{\text{struct}}(\vec{r})}{E_0(\vec{r})}\right)^2 = \frac{n_{\text{struct}}(\vec{r})}{n_0} \times \left(\frac{|E_{\text{struct},c}(\vec{r})|}{|E_{0,c}(\vec{r})|}\right)^2, \tag{4}$$

where $E_{\text{struct},c}, E_{0,c} \in \mathbb{C}$ are the electric field components in their complex form, n_{struct} describes the refractive index within the structure at position $\vec{r}$ and n_0 is the refractive index of 1.5 of the reference simulation.

2.3. The variation of the local density of photonic states

The second effect of photonic structures on upconversion processes is the variation of the local density of photonic states (LDOS) at the transition frequencies. Fermi's golden rule [45] states that the transition probability P_{if} of a spontaneous emission process at the frequency ω_{if} between the ionic states of the upconverter ion 'i' and 'f' is proportional to the local density of photonic states $\rho(\vec{r}, \omega_{if})$ at the emission frequency ω_{if} and position $\vec{r}$:

$$P_{if}(\vec{r}) = \frac{2\pi}{\hbar} |M_{if}|^2 \rho(\vec{r}, \omega_{if}), \tag{5}$$

with the transition matrix element M_{if}.

Therefore, emission within a photonic band gap is inhibited whereas the emission around the band gap can be increased [22]. The factor $\gamma_{if}(\vec{r})$ represents the change of the probability of a spontaneous emission process between the two states 'i' and 'f'due to the photonic structure. It can be expressed by the change of the local density of photonic states:

$$\gamma_{if}(\vec{r}) = \frac{P_{if,\text{struct}}(\vec{r})}{P_{if,0}(\vec{r})} = \frac{\rho_{\text{struct}}(\omega_{if}, \vec{r})}{\rho_0(\omega_{if}, \vec{r})}, \tag{6}$$

where again the index 'struct' denotes the quantities with the photonic structure and '0' the case in a homogeneous medium with a refractive index of $n_0 = 1.5$.

Due to the effect of the varied LDOS, the spontaneous emission at each frequency and position can be either enhanced or suppressed. In principle, this offers the opportunity to tune the transition rates in order to increase the upconversion quantum yield.

For the specific upconverter material β-$NaYF_4$ doped with 20% Er^{3+}, the dominant upconversion emission at 980 nm should be enhanced, while other unwanted transitions, for example the spontaneous emission from the first excited state at a wavelength of 1523 nm should be suppressed.

#192534 - $15.00 USD Received 18 Jun 2013; revised 21 Jul 2013; accepted 21 Jul 2013; published 28 Aug 2013

2.4. Simulation of the variation of the local density of states

To determine the change factor $\gamma_{if}(\vec{r})$ of the LDOS due to the photonic structure at the transition frequencies, we again used an FDTD simulation. In contrast to the previous case, where a line source was placed outside the waveguide structure, this time a point dipole emitter inside the structure was simulated [46–48]. Additionally, the emission is no longer monochromatic at a wavelength of 1523 nm, but has a Gaussian shape in the frequency domain. The Gaussian shape offers the opportunity to cover a certain frequency range with each simulation run.

The emission of a Gaussian pulse in the frequency domain implies a Gaussian-modulated sine wave at the center frequency in the time-domain.

The point dipole source is surrounded by four detector planes as sketched in Fig. 2. Meep, the simulation software used here, allows for direct recording of the Poynting vector $\vec{S}$ in the frequency domain over the area $\vec{A}$ of these flux detection planes. The emitted energy is measured in these detector planes as the waves pass through, and the simulation program directly performs a Fourier-transformation on this data. Thus, after the simulation run, the emitted energy $W(\omega_{if},\vec{r})$ is obtained spectrally resolved according to

$$W(\omega_{if},\vec{r}) = \frac{\partial \int_A \vec{S}(\omega,\vec{r}) d^2\vec{r}}{\partial \omega}|_{\omega_{if}} \Delta\omega, \tag{7}$$

In principle, this method has been demonstrated in [46]. The emitted energy is thereby proportional to the local density of photonic states. Thus, the LDOS can be deduced from this data.

Inside the photonic structure environment, the initially Gaussian shape of the emission is distorted. The emitted energy W at the transition frequencies ω_{if} is proportional to the local density of photonic states ρ at this frequency. Thus, the relative enhancement factor for this frequency $\gamma_{if}(\omega_{if})$ can be obtained by dividing the emitted energy at the transition frequencies $W_{\text{struct}}(\omega_{if})$ by the corresponding unperturbed values taken from a reference simulation in a homogeneous medium of refractive index $n_0 = 1.5$.

$$\gamma_{if}(\vec{r}) = \frac{W_{\text{struct}}(\omega_{if},\vec{r})}{W_0(\omega_{if},\vec{r})}. \tag{8}$$

As the LDOS is a local quantity, this procedure has to be repeated for each position within the simulated structure. In the case of our waveguide structure, the inner area of the waveguide was covered by $384 (19 \times 24)$ lattice points.

For these simulations, the simulation cell had to be extended in the x-direction for several periods, compared to the previously used where only one period of the structure was simulated with periodic boundaries. Here, periodic boundaries would imply that field components leaving in x direction re-entered the simulation cell from the +x direction and would be count in the detector planes, leading to wrong results. The simulation results shown in this paper were obtained in simulation runs covering 50 periods of the waveguide structure followed by a PML.

Furthermore, at each lattice point the emission has to be simulated for all possible dipole orientations. The dipole can be oriented along the x-axis, the y-axis or perpendicular to the simulation cell. The simulation is set in two dimensions, thus, the structure is taken to be infinitely extended in z-direction. This is a simplification, which has become necessary to limit the calculation time to an acceptable range. In principle these effects should be simulated in a three-dimensional setup. Because one dimension, in which no specific structure is present, has been omitted, the following results overestimate the impact of the waveguide structure. However, this does not influence the validity of the simulation approach shown here, which could be applied to a three-dimensional setup as well. It is expected that the simulated effects occur less pronounced in an actual measurement.

#192534 - $15.00 USD Received 18 Jun 2013; revised 21 Jul 2013; accepted 21 Jul 2013; published 28 Aug 2013

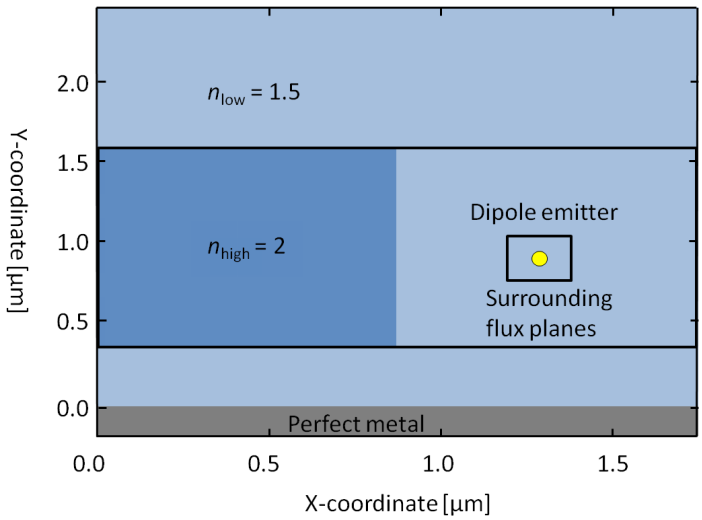

Fig. 2. Simulation setup for the evaluation of the transition enhancement factor. The grating part of the structure (black box) is investigated in the following.

2.5. *Simulating the upconverter material*

As mentioned already in the introduction, β-$NaYF_4$ doped with Er^{3+} is known to be one of the most efficient materials for upconversion of photons from the near infrared to energies above the band gap of silicon [42]. Therefore, in this paper, we concentrate our analysis on this material. The trivalent erbium in this material features distinct energy levels that form an energy-ladder, which can be excited in the infrared at a wavelength of around 1523 nm (see Fig. 3). Subsequent absorption of photons or energy transfer between neighboring ions can lead to the emission of higher-energy photons. The most frequent emission occurs at a wavelength of 980 nm. These photons can be utilized in a silicon solar cell.

A model describing the dynamics of the upconversion processes in this material has been published in [49,50]. This model describes the absorption, emission, energy transfer, and multi-phonon relaxation processes in β-$NaYF_4$: 20% Er^{3+}. All relevant transitions for the upconversion of infrared photons at a wavelength of 1523 nm within a trivalent erbium ion are considered in this model which is based on rate equations. The occupation of the six lowest energy levels as shown in Fig. 3 is described by an occupation vector $\vec{n}$. The individual elements of the vector are the relative occupation of the specific energy level, i.e. the fraction of ions of a large ion ensemble that is excited to this state.

The occupation vector $\vec{n}$ and its rate of change $\dot{\vec{n}}$ are described by the differential equation:

$$\dot{\vec{n}} = [GSA + ESA + STE + SPE + MPR] \times \vec{n} + \vec{v}_{ET}(\vec{n}). \tag{9}$$

The processes linear to the occupation vector $\vec{n}$ are described by matrices. The matrix GSA describes the ground state absorption, ESA the excited state absorption, STE the stimulated emission, SPE the spontaneous emission and MPR the multi-phonon relaxation processes. Energy transfer processes $\vec{v}_{ET}(\vec{n})$ which are not linear in $\vec{n}$ are described by a set of vectors [50]. The model is based on experimentally determined Einstein coefficients of the radiative transitions involved [49, 50]. From these, the matrix entries for GSA, ESA, STE and SPE are determined, together with some factors such as the incident photon flux density, in the case of the

#192534 - $15.00 USD Received 18 Jun 2013; revised 21 Jul 2013; accepted 21 Jul 2013; published 28 Aug 2013

stimulated processes.

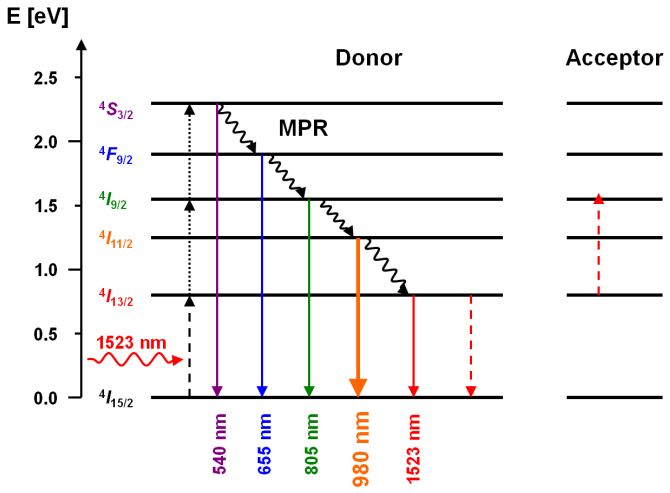

Fig. 3. Energy level diagram of Er^{3+} in the host crystal β-$NaYF_4$. The ion is excited at a wavelength of 1523 nm. Higher states are occupied either by subsequent absorption of photons (black broken arrows) or energy transfer processes (red broken arrow). The waved arrows depict multi-phonon relaxation processes [49, 50].

As outlined at the beginning of this section, the stimulated processes are scaled by the factor $\gamma_E(\vec{r})$ by which the incident photon flux at the position of the upconverter is modified (see Eq. (1)). For taking into account the modified LDOS, the Einstein coefficients for the spontaneous emission from the various levels are scaled by the factor $\gamma_{if}(\vec{r})$:

$$A_{if,\text{struct}}(\vec{r}) = \gamma_{if}(\vec{r}) \times A_{if}. \tag{10}$$

The absorption and stimulated emission rates are considered to be independent of the transition enhancement factor $\gamma_{if}(\vec{r})$, as according to Fermi's golden rule only the density of final states has to be taken into account. In the absorption case, the final states are electronic states which are independent of the photonic LDOS.

Whether energy transfer processes between the erbium ions are significantly influenced by the change of the LDOS is under heavy debate in literature [51–53]. In this work the energy transfer processes are considered to be independent of the LDOS. Therein we follow the theoretical reasoning presented in [51], which states that the very short lifetime of the virtual photons involved in the energy transfer corresponds to a very broad energy range, thus, the effect of the LDOS at a specific theoretically determined transition wavelength plays a negligible role. However, as this appears to be an open question, we also performed calculations assuming the other case: a linear influence of the changed LDOS on the donor ion. The according results will be briefly compared to our main findings.

Considering the variations due to the photonic structure, the rate equation model can be used to simulate the absorption and luminescence of the upconverting material within a photonic structure environment. The absorption rate *Abs* is determined as the sum over *GSA* and *ESA* processes from the initial state minus the *STE* from excited states, thus all processes occurring at the incident wavelength of 1523 nm [50]. The matrices are multiplied by the occupation of the corresponding energy levels, where $\vec{n}(1)$ describes the occupation of the $^4I_{15/2}$ ground state,

#192534 - $15.00 USD Received 18 Jun 2013; revised 21 Jul 2013; accepted 21 Jul 2013; published 28 Aug 2013

$\vec{n}(2)$ describes the occupation of the ${}^4I_{13/2}$ first excited state and so on.

$$\begin{aligned} Abs = \vec{n}(1) \times GSA + \vec{n}(2) \times ESA + \vec{n}(4) \times ESA \\ - \vec{n}(2) \times STE - \vec{n}(4) \times STE - \vec{n}(6) \times STE. \end{aligned} \tag{11}$$

The absorption enhancement γ_{Abs} is defined as:

$$\gamma_{\mathrm{Abs}} = \frac{Abs_{\mathrm{struct}}}{Abs_0}. \tag{12}$$

The luminescence rate of a specific transition is the population of the starting energy level times the spontaneous emission Einstein coefficient for the specific transition [50]. For the following considerations, only the luminescence rate *Lum* from the ${}^4I_{11/2}$-level to the ground state is considered as this corresponds to the by far most frequent upconversion emission process [7] in β-$NaYF_4$: 20% Er^{3+}:

$$Lum = \vec{n}(3) \times A_{31}. \tag{13}$$

The luminescence enhancement γ_{Lum} is defined as:

$$\gamma_{\mathrm{Lum}} = \frac{Lum_{\mathrm{struct}}}{Lum_0}. \tag{14}$$

The absorption rate and the luminescence rate can subsequently be used to determine a quantum yield for each lattice position. The mean UCQY for the whole structure is determined according to:

$$UCQY = \frac{\sum_{\vec{r}} Lum}{\sum_{\vec{r}} Abs}. \tag{15}$$

The summation is carried out over the grating part of the structure only. The quantum yield can subsequently be related to the quantum yield of the unchanged upconverter system $UCQY_0$, and an enhancement factor γ_{UCQY} for the upconversion quantum yield can be obtained:

$$\gamma_{\mathrm{UCQY}} = \frac{UCQY_{\mathrm{struct}}}{UCQY_0}. \tag{16}$$

We assume linear optics, thus, the irradiance enhancement and the change of local photon density are taken to be independent from the starting irradiance. However, the overall quantum yield, as well as the enhancement factor for the quantum yield depends on the irradiance, which reaches the unmodified upconverter or the whole upconverter/photonic structure system, respectively. This increase of upconversion quantum yield saturates for higher irradiance values [7, 49]. In this paper, we assume a starting irradiance of 200 Wm^{-2}, corresponding to a photon flux of $1.5 * 10^{21}$ $\mathrm{s}^{-1}\mathrm{m}^{-2}$ of photons with a wavelength of 1523 nm. The value of 200 Wm^{-2} could be reached by spectral [54, 55] and geometric concentration as in the AM1.5 spectrum only a fraction of this energy is carried by photons in a wavelength range around 1523 nm. The absorption range of β-$NaYF_4$: 20% Er^{3+} extends from around 1480 nm to 1580 nm [7]. In this region an irradiance of 23 Wm^{-2} is found, thus, the irradiance of 200 Wm^{-2} could be reached at a geometric concentration of a factor of around 9 without additional spectral concentration. If one would only assume absorption of laser light, with a spectral width of 1 nm, the equivalent solar concentration would increase to approximately 700 suns.

#192534 - $15.00 USD Received 18 Jun 2013; revised 21 Jul 2013; accepted 21 Jul 2013; published 28 Aug 2013

3. Results

To optimize the geometry of the waveguide structure, in a first step, the irradiance enhancement was determined for a set of structures, as described in Section II.B. The irradiance distribution was obtained within each structure. This irradiance distribution was taken as an input for the rate equation model. With this input a preliminary effect of the photonic structure on the UCQY could be determined, which is purely based on the irradiance enhancement and neglects the influence of the variation of the local density of states. This was done, to keep computation times within reasonable limits.

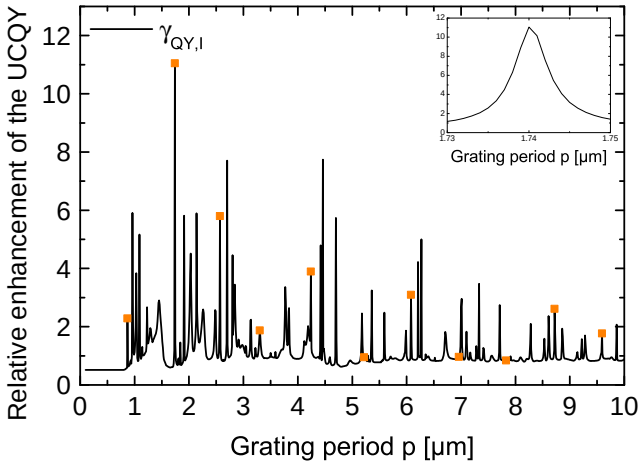

Fig. 4. Enhancement of the upconversion quantum yield due to the irradiance enhancement within the structure. A first, dominant maximum is obtained for a grating period of 1.74 μm indicating a QY enhancement of a factor of 11. The inset shows the peak shape of this maximum. The orange squares denote integer multiples of 0.87 μm. This period corresponds to a resonance of the grating part of the structure.

Figure 4 shows, as an example, the optimization of the structure period p. The structure period p was varied from 0.1 μm to 10 μm. The orange squares in the plot denote integer multiples of a period of 0.87 μm. These periods corresponds to a high incoupling efficiency of the grating for light with a wavlength of 1523 nm into a waveguide with a refractive index of 1.75, the effective refractive index of the grating area of the structure. Due to the complexity of the investigated structure, more peaks evolve due to resonances in the different layers. These various resonances can interfere constructively or destructively leading to the very complex pattern shown. All other structure parameters (the thickness of the buffer layer between the mirror and the grating, the grating thickness and the thickness of the top layer) were optimized in a similar manner (not shown). The fill factor of the grating was kept constant at 50%. Thus, the structure with the most beneficial irradiance distribution at the incident wavelength of 1523 nm could be determined.

A first maximum in the preliminary enhancement factors $\gamma_{QY,I}$ is obtained for a structure period of 1.74 μm. Additionally, the peak at a period of 2.7 μm was investigated further. These two structure periods are expected to show very different effects on the LDOS. For the first structure with a period of 1.74 μm, the one-dimensional band structure that can be associated with the grating part of the structure shows a band gap at the absorption wavelength of 1523 nm,

#192534 - $15.00 USD Received 18 Jun 2013; revised 21 Jul 2013; accepted 21 Jul 2013; published 28 Aug 2013

while the emission wavelength of 980 nm is located close to a band edge. This results in an enhancement of the density of states at the emission wavelength. If we look at the corresponding one-dimensional band structure of the second maximum at a period of 2.7 μm, the absorption wavelength is found close to the band edge whereas the emission wavelength is hardly affected. This was taken as a simple qualitative indicator that the structure period of 1.74 μm could be more beneficial to the upconversion quantum yield than the larger period of 2.7 μm.

These two preliminarily optimized geometries were then used to carry out a complete simulation considering all described effects. For the structure with the larger period of 2.7 μm, the resulting upconversion quantum yield was only 26% of the value without a waveguide structure under an initial irradiance of 200 Wm^{-2}. Surprisingly, the UCQY was decreased despite of the irradiance enhancement. The reason was that the strong enhancement of the irradiance at 1523 nm correlates with an enhancement of the local density of states at the same wavelength. Hence, simultaneously to the enhancement of the irradiance, the probability for direct re-emission of absorbed photons increases. Thus, photons excited to the first excited level directly relax back to the ground state re-emitting a photon at a wavelength of around 1523 nm. Hence, the population of the first excited level decreases. A rather strong impact of this effect within the model was observed that ultimately limits the upconversion quantum yield. Thus, here we show the results for the first structure period of 1.74 μm.

Figure 5 shows the spatial distribution of the irradiance enhancement over the grating region illuminated by the combined TE- and TM-source for the structure presented in Fig. 1.

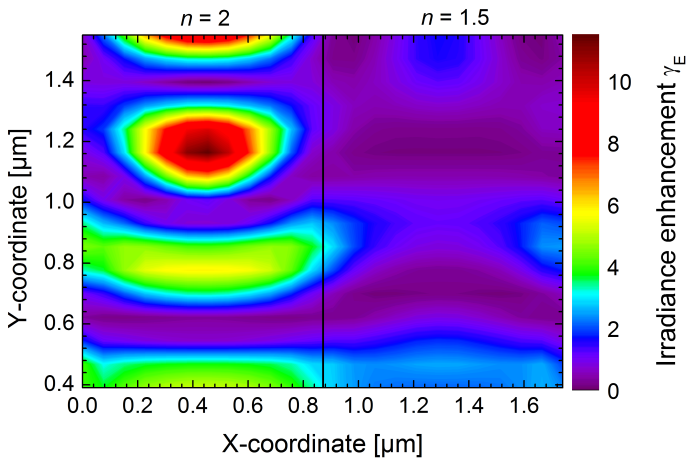

Fig. 5. Enhancement factor γ_E of the local irradiance within the grating structure for a grating period of 1.74 μm. The graph shows the grating part of the structure as indicated by the box in Fig. 2. Within the grating region, the irradiance can be increased by up to a factor of 11.5 in the high-index region (left) and up to a factor of 2.9 in the low-index region (right).

As one can see in Fig. 5, the irradiance can be increased considerably in the optimized waveguide. This effect concentrates on the high-index region where enhancement factors γ_E of up to 11.5 are reached. Thus, it would be advantageous to have upconverting host materials with high refractive index. In the low-index region, an enhancement factor of up to 2.9 was achieved. The average enhancement factor for the whole waveguide is 2.0. Subsequently, a simulation considering all effects and especially the varied LDOS was performed.

#192534 - $15.00 USD Received 18 Jun 2013; revised 21 Jul 2013; accepted 21 Jul 2013; published 28 Aug 2013

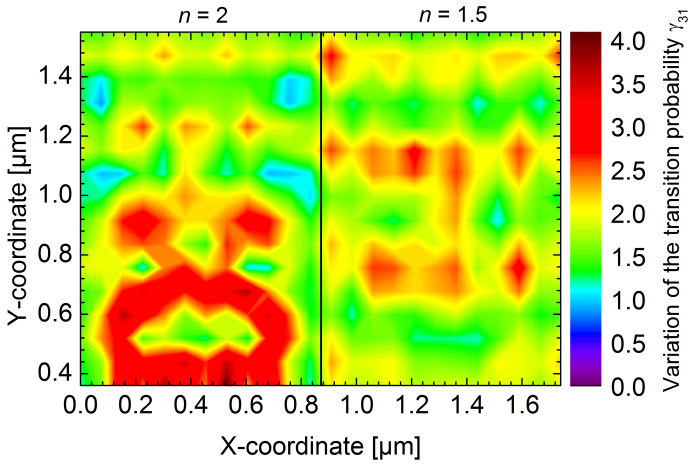

Fig. 6. Variation of the transition probability γ_{31} for the transition from the $^4I_{11/2}$ level to the ground state. The grating part of the structure is shown, with the high-index region on the left and the low-index region on the right. One can see that in the high-refractive index region (left), enhancement factors of the transition rate between 0.9 and 4.1 are found. In the low-index region (right), factors between 1.1 and 2.9 are reached.

The enhancement factors for the transition rates were determined according to the description in Section II.D. This has been done for each transition frequency of the electronic transitions within the erbium ion that are included in the rate equation model.

The spatial distribution of the enhancement factor for the emission transition from $^4I_{11/2}$ to the ground state is shown in Fig. 6. The transition rate can be enhanced by up to a factor of 4.1 in the high-index region and up to a factor of 2.9 in the low-index region. The transition rate is not decreased at all in the low-index region and only at very small spots in the high-index region. Thus, the emission probability of a photon at a wavelength of 980 nm is considerably increased over the whole structure.

The results from the simulation of the photon flux enhancement as well as the variation factors for all the different transitions were subsequently integrated into the rate equation model of the upconverter.

Figure 7 shows the enhancement of the luminescence from the $^4I_{11/2}$ -level as determined from the rate equation model according to Eq. (15). In the high-index region, the luminescence can be increased by up to a factor of 30.0, whereas in the low-index region, peak enhancement values of 4.0 can be reached. Averaged over all lattice points the luminescence increases by a factor of 3.3. This increase of the luminescence is caused to a large extent by an increased absorption, as shown in Fig. 8. A maximum absorption enhancement factor of 10.0 occurs in the high-index region, and a maximum absorption enhancement factor of 2.8 is observed in the low-index region. Comparing Fig. 7 and Fig. 8 shows a clear correlation between the luminescence enhancement and the absorption enhancement. Thus, a great part of the luminescence enhancement is simply due to more absorption.

From the luminescence and the absorption, the UCQY can be calculated according to Eq. (15).

As depicted in Fig. 9, the investigated waveguide structure leads to enhancement factors for the UCQY of up to 3.9. The overall UCQY improves by a factor of $\gamma_{\mathrm{UCQY}} = 1.8$ under the

#192534 - $15.00 USD Received 18 Jun 2013; revised 21 Jul 2013; accepted 21 Jul 2013; published 28 Aug 2013

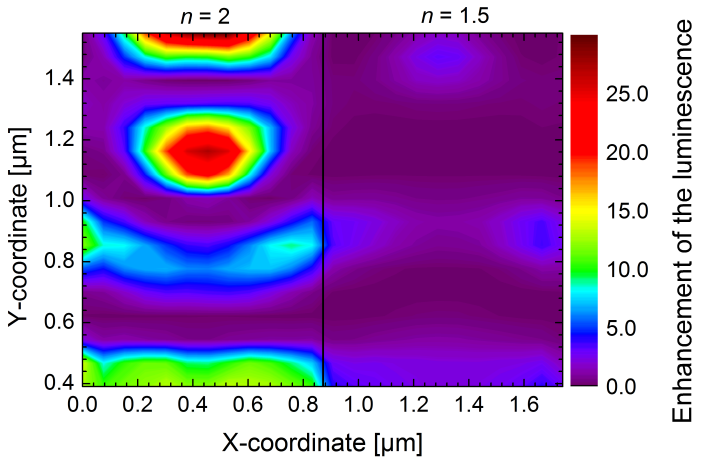

Fig. 7. Enhancement of the luminescence for an initial irradiance of 200 Wm^{-2}. The luminescence can be increased by up to a factor of 30.0 in the high-index region (left) and up to a factor of 4.0 in the low-index region (right).

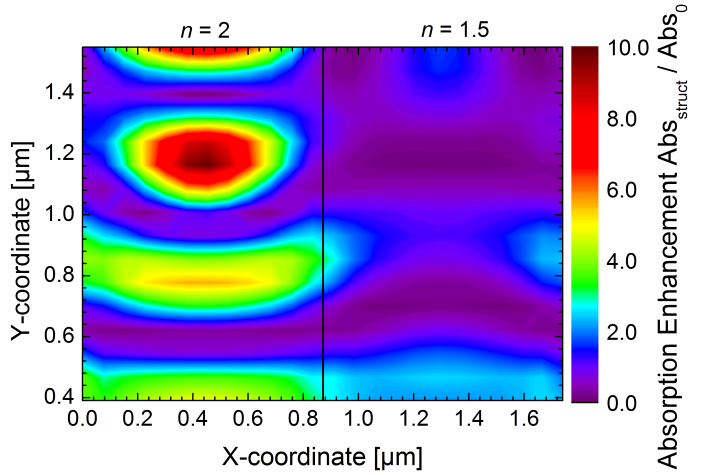

Fig. 8. Enhancement of the absorption of the incident irradiance at a wavelength of 1523 nm. The absorption is increased by up to a factor of 10.0 in the high-index region (left) at the same spots, where the highest luminescence values are found. In the low-index region (right), the absorption enhancement is smaller, with a maximum enhancement of 2.8.

#192534 - $15.00 USD Received 18 Jun 2013; revised 21 Jul 2013; accepted 21 Jul 2013; published 28 Aug 2013

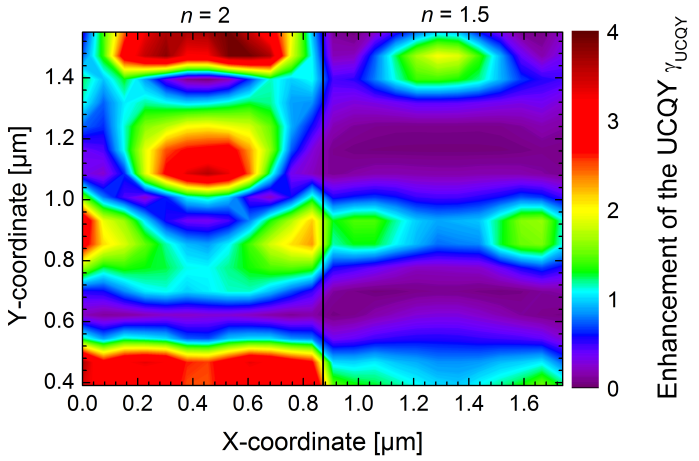

Fig. 9. Relative upconversion quantum yield enhancement at each lattice position for the transition from the $^4I_{11/2}$ level to the ground state $^4I_{15/2}$. The initial irradiance without the structure was set to be 200 Wm^{-2}. A maximum relative enhancement of the upconversion quantum yield by a factor of 3.9 can be reached. In the low-index region (right), peak enhancement values of 2.0 can be found. Over the whole structure, the UCQY is increased by a factor of 1.8.

assumption that the upconverter material is evenly distributed within the whole grating region. Table 1 gives an overview over the different enhancement factors.

Table 1. Overview over maximum and averaged enhancement factors of the determined different quantities within the waveguide structure: The maximum values are given for the low and high refractive index region separately; the average was calculated for the whole structure

	γ_E	γ_{tf}	γ_{Lum}	γ_{Abs}	γ_{UCQY}
max_{low}	2.9	2.9	4.0	2.8	2.0
max_{high}	11.5	4.1	30.0	10.0	3.9
average	2.0	1.9	3.3	1.9	1.8

When the same analysis is carried out with an assumed linear influence of the changed LDOS on the energy transfer processes, an overall increase of the upconversion quantum yield by a factor of 3.3 is obtained. This higher increase is not surprising, as energy transfer upconversion is the dominating upconversion process in β-$NaYF_4$ doped with Er^{3+}. Thus any changes in the energy transfer strongly influence the UCQY.

4. Discussion and conclusion

From the obtained results, it can be concluded that embedding the upconverter material in a suitable photonic structure has the potential to enhance the upconversion luminescence and quantum yield. The absolute enhancement factors, however, must be interpreted with care, as the simulations have been carried out in a two-dimensional setup.

#192534 - $15.00 USD Received 18 Jun 2013; revised 21 Jul 2013; accepted 21 Jul 2013; published 28 Aug 2013

We find that the overall luminescence of the structure could be 3.3 times higher than within a homogenous medium, which is mainly attributed to an increased absorption. In an application, this would mean that a much stronger upconversion signal from the same amount of material could be achieved, or that less material is needed for the same signal strength. In a solar cell, this would eliminate the need for more than one mm thick layers of upconverter material, which had been necessary to achieve a significant impact of the upconverter in previous works [8, 9].

For the photovoltaic application, however, the limiting factor has not been the overall luminescence, but the overall low UCQY, that is, the fraction of luminescence divided by the absorption. Here, the quantum yield could be increased by a factor of 1.8.

This work also shows that it is necessary to consider all effects, in expression the field enhancement and the varying local density of photonic states. One of our structures chosen due to a high irradiance enhancement, actually resulted in a reduced mean upconversion quantum yield.

There are, however, also certain limitations to our results. Several simplifications were made in the course of the presented work, in order to reduce the complexity of the model. Some of them tend to overestimate the impact of the photonic structure on an increase of the QY: first, the fact that the structure is simulated in a two-dimensional setup instead of three-dimensional space. This leads to an over-estimation of the confinement effects within the photonic structure. On the other hand, an additional confinement could be achieved for a two-dimensional grating structure, this has been shown for distributed feedback lasers [56, 57]. Second, the simulation procedure does not consider absorption by the upconverter material, when calculating the irradiance distribution. Thus, at some places of the structure the actual irradiance the upconverter experiences would be lower, although this is only a small effect. Additionally, the rate equation model is based on the upconversion properties of microcrystalline β-$NaYF_4$ doped with 20% Er^{3+}. Although, the crystal-size of this upconverter material is actually too large to be incorporated in a photonic structure, the effects on nanocrystalline material are expected to be similar.

On the other hand, re-emission from the $^4I_{11/2}$ level to the ground state is neglected, which could lead to "photon-recycling", by another absorption process. In average around 98% of the absorbed photons are directly re-emitted, with a wavelength similar to the excitation. It is obvious that photon recycling can increase the overall upconversion quantum yield. Another neglected effect, which could lead to an underestimation of the impact of the photonic structure, is the possibility for stimulated emission from the desired transitions stimulated by upconverted photons previously emitted.

Even if at the bottom line, the obtained results slightly overestimate the potential, the possible enhancements are still promising. This becomes apparent, when the determined results are compared to other strategies for increasing the upconversion processes in the most efficient upconverting material of erbium-doped β-$NaYF_4$. For example, Hallermann et al. found a potential increase of 20% in the overall luminescence for the combination of the same upconverter material investigated in our paper with a metallic nanoparticle [12]. In that study, a highly idealized model for the effect of the nanoparticle has been used. This model was coupled with the same upconverter model used for our study. The overall increase of 20% has to be compared to our findings of a potential 3.3-fold increase. In experiments, Schietinger et al. found a luminescence increase by a factor of 3.8 for a single upconversion particle in the proximity of a metallic nanoparticle [16], which was placed at an ideal position to achieve a maximum impact. This compares to the peak values of a 30-fold increase for the local luminescence increase in the low-index region of our structure. The better performance of the structure investigated in this paper can be understood considering the major advantage of using dielectric nanostructures instead of plasmon resonances around metallic nanoparticles, which is that no additional

#192534 - $15.00 USD Received 18 Jun 2013; revised 21 Jul 2013; accepted 21 Jul 2013; published 28 Aug 2013

non-radiative decay paths are introduced by the nanostructures.

As a next step, it is now necessary to confirm the promising potential of the investigated structure in quantitative measurements of the upconversion luminescence, as up to now, only photoluminescence measurements and no quantum yield measurements could be found in literature for experimentally realized combinations of photonic structures with upconverter material.

5. Summary

In this paper we presented a comprehensive theoretical model describing the impact of photonic structures on upconversion. The model considers the effects of a change of the local irradiance due to the structure and the effects of a variation of the local density of photonic states on the processes within the upconverter of ground state absorption, excited state absorption, stimulated emission, spontaneous emission, multi-phonon relaxation and energy transfer processes. To our knowledge, this work presents the first combined theoretical analysis of photonic structures and their effect on upconversion processes relying on multiple absorption or energy transfer processes. The theoretical model was subsequently implemented into a simulation tool. With this simulation, it was shown that an optimized waveguide structure can increase the overall luminescence by a factor of 3.3 and the overall quantum yield by a factor of 1.8. The upconverter material of β-$NaYF_4$:20%Er^{3+} used here shows an UCQY of 0.86% [7] at an initial irradiance of 200 Wm^{-2}. This value could be increased by embedding the upconverter into a photonic waveguide structure to 1.5%. The key to the successful optimization of the structure was to increase the local density of photonic states at the frequencies corresponding to the transitions inside the erbium ion.

The results shown here may not be the final limit as a complete optimization of the structure parameters for a maximum quantum yield enhancement was beyond the scope of this paper. Ideally, such an optimization would include the whole solar cell upconverter device instead of only the upconverter.

We discussed that the potential increase in the UCQY is considerably higher than what can be achieved with alternative strategies, so far. Such an increase would be extremely helpful in applications of upconversion, as in photovoltaics.

Acknowledgment

The authors would like to thank Oliver Höhn for fruitful discussions. The research leading to these results has received funding from the German Federal Ministry of Education and Research in the project "InfraVolt Infrarot Optische Nanostrukturen für die Photovoltaik" (BMBF, project number 03SF0401B), and from the European Community's Seventh Framework Programme (FP7/2007-2013) under grant agreement n[246200]. S. Fischer gratefully acknowledges the scholarship support from the Deutsche Bundesstiftung Umwelt DBU, J. Gutmann gratefully acknowledges the scholarship support from the Reiner Lemoine Stiftung and J. C. Goldschmidt acknowledges the support by the German Academic Exchange Service (DAAD).